XI. COGNITIVE INFORMATION PROCESSING*

Academic and Research Staff

Prof. M. Eden
Prof. J. Allen
Prof. B. A. Blesser
Prof. T. S. Huang
Prof. F. F. Lee
Prof. S. J. Mason
Prof. W. F. Schreiber
Prof. D. E. Troxel
Prof. I. T. Young
Dr. R. R. Archer
Dr. J. E. Green
Dr. K. R. Ingham
Dr. D. M. Ozonoff
Dr. D. A. Sankowsky
Dr. O. J. Tretiak
F. X. Carroll
C. L. Fontaine
E. R. Jensen
E. Peper
Sandra A. Sommers

Graduate Students

T. P. Barnwell III
W. L. Bass
T. R. Bourk
J. E. Bowie
B. E. Boyle
R. L. Brenner
S. A. Ellias
J. R. Ellis, Jr.
A. E. Filip
R. E. Greenwood
W. B. Grossman
E. G. Guttmann
D. W. Hartman
L. Hatfield
L. P. A. Henckels
P. D. Henshaw
M. Hubelbank
J. I. Makhoul
G. P. Marston
G. G. Matison
W. McCandless
G. F. Pfister
D. S. Prerau
N. Rashid
G. M. Robbins
C. L. Seitz
R. D. Shapiro
R. D. Solomon
W. W. Stallings
K. P. Wacks
G. A. Walpert
T. R. Willemain
Y. D. Willems

A. ANALYZING THE PERFORMANCE OF AN IMAGE-PROCESSING SYSTEM

This report summarizes an E. E. thesis with the same title that was submitted to the Department of Electrical Engineering, M. I. T., in June 1970.

Research has been conducted to establish a method for measuring the performance of an image-transmission system. The measurement criterion used in current research is the subjective response of observers. This involves not only properties of the image, which are usually quantitative, but also the physiology of human vision and the psychology of human perception. These human factors, jointly termed psychophysics, are usually discussed qualitatively and hence have led to imprecise analyses of the performance of image-processing systems. The approach used to control and measure the effects of those parameters that affect human response in an experimental image-transmission system will be outlined.

Two image-transmission systems were computer simulated. One, called the "standard" system, was a variant of pulse code modulation[1] which involved relatively simple pre- and post-transmission coding techniques, while the other, called the "Experimental" system, implemented more sophisticated methods to reduce the amount of data to be

*This work was supported principally by the National Institutes of Health (Grants 5 PO1 GM14940-04 and 5 PO1 GM15006-03), and in part by the Joint Services Electronics Programs (U.S. Army, U.S. Navy, and U.S. Air Force) under Contract DA 28-043-AMC-02536(E).

transmitted. The fundamental parameters in both systems were the number of samples per picture ($S \times S$) and the number of quantization levels (2^{QC}) per sample. The total number of binary digits needed to represent the picture is then $C = S \times S \times QC$, where C could be the capacity (in bits) of an available communication channel. The essential measurement was made on the relation of C for the Standard system to C for the Experimental system when both systems transmitted images of the same quality. The variation of this performance factor, called the "compression ratio," as a function of C for the Standard system and the subject matter of the picture transmitted, was studied.

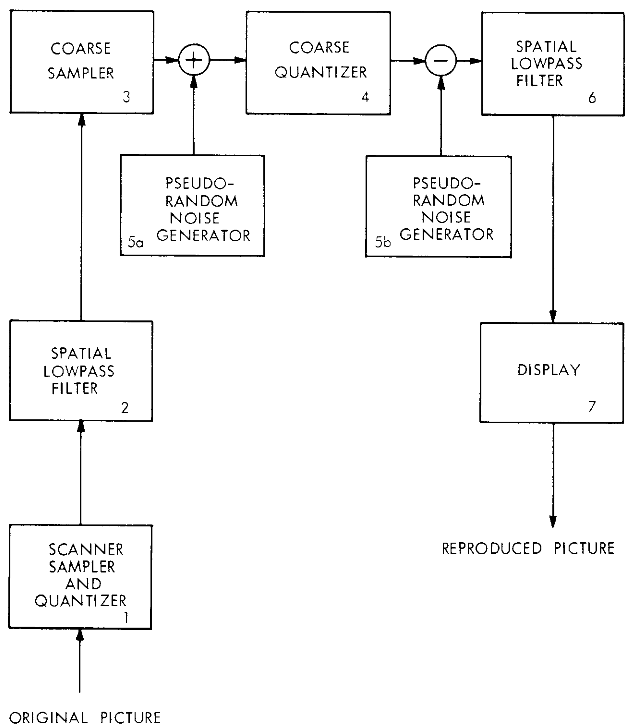

Fig. XI-1. Standard system.

The method for producing the set of pictures to serve as standards of comparison is shown in Fig. XI-1. This implementation represents a compromise between the desire to find a very simple method to convey an image in C bits, and yet not produce such a distorted result that viewers would in most cases be overly biased in favor of the Experimental system. With reference to Fig. XI-1, blocks 2 through 5a constitute the source coder. The output of block 1 is an $N \times N$ array of samples, each comprising QF bits (mnemonic for quantized finely). The object of the source coder is to compress the information content of these $N \times N \times QF$ bits into an array of $S \times S$ samples, each composed of QC bits (mnemonic for quantized coarsely), so $S \times S \times QC = C$. The source decoder that comprises blocks 5b and 6 performs the reverse operation.

The digital scanner and display, blocks 1 and 7, are embodied in a laboratory device built by the Cognitive Information Processing Group of the Research Laboratory of Electronics. Using a flying-spot scanner, this device records sample values from a transparency, quantizes each sample into one of 256 uniformly spaced brightness levels, and records the resulting numbers in binary form on magnetic tape in a format compatible with the IBM 360 computer. Figure XI-2a is a picture produced by the scanner with $N = 256$ and $QF = 8$.

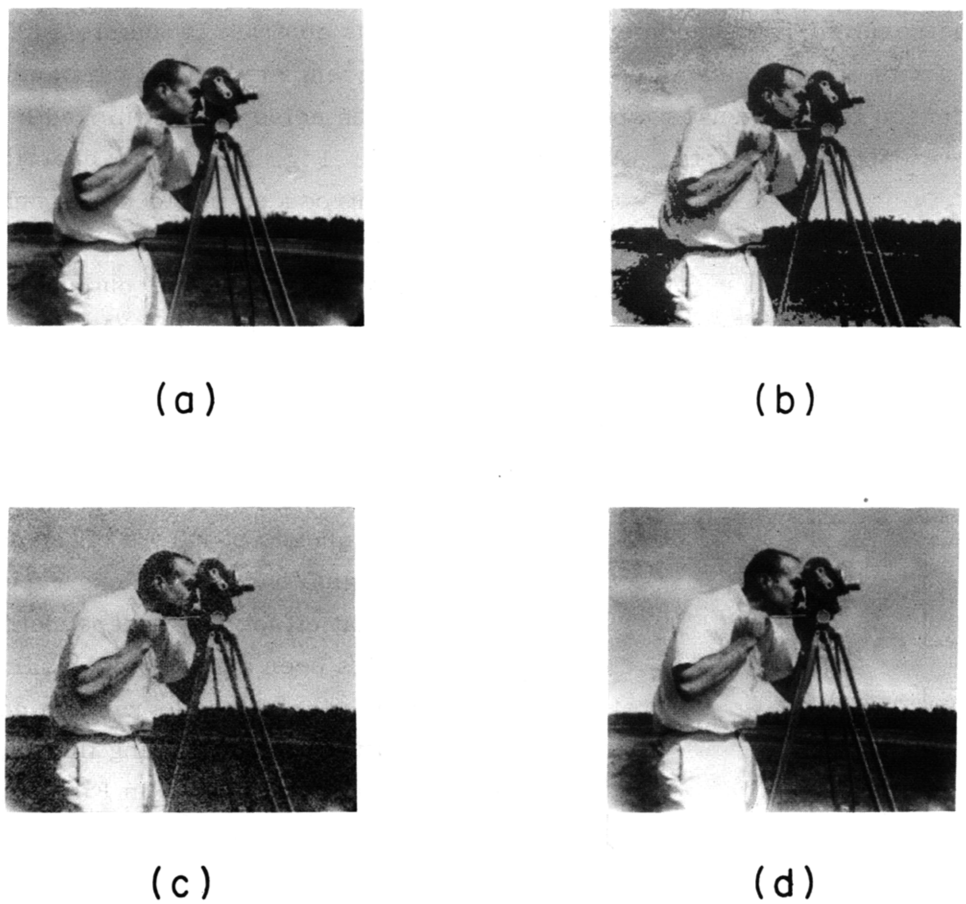

Fig. XI-2. Coarse quantizing techniques.

Now that the image is in digital form the next few stages compress the picture information into $S \times S$ samples, each quantized to 2^{QC} levels. Blocks 2 and 6 are linear filters that act on the two-dimensional array of samples so that the number of samples can be reduced without introducing much error. Petersen and Middleton have proved[2] that the minimum mean-square error between an n-dimensional function and its recreation from a square lattice of sample values is obtained if the function is bandlimited up to spatial frequencies equal to one-half the sampling rate before sampling and again before reconstruction. This is a statement analogous to the one-dimensional sampling theorem. The use of such filters in blocks 2 and 6 produced visible spurious artifacts, called "ringing," which are attributable to the Gibbs phenomenon. These effects were eliminated by using a Gaussian lowpass filter in block 2 and linear interpolation in block 6. The most direct method of reducing the number of bits per sample for all $S \times S$ samples from QF to QC would be to map the 2^{QF} fine divisions into the nearest of the 2^{QC} divisions. This scheme, known as pulse code modulation (PCM), was tested with QC = 3, QF = 8 (note that QF = 8 for all pictures in this report), N = 256 and S = 256. Figure XI-2b shows the results. The phenomenon of simultaneous contrast is manifest here; the boundaries of areas of equal quantized brightness are accentuated. This particularly annoying effect, caused by the visual response to quantization noise, was removed by using a technique developed by Roberts.[3] As diagrammed in Fig. XI-1, the quantization noise introduced in block 4 is converted into random noise, commonly called "snow," by adding to the output of block 3 a deterministic signal whose amplitude varies over plus or minus one-half of a coarse quantization level from sample to sample and by subtracting the identical signal after quantization. The sequence of values of the deterministic signal has such a long repetition time that effectively independent random noise has been added to each sample; hence, the term pseudo-random noise. A picture produced using this method with QC = 3 is shown in Fig. XI-2c.

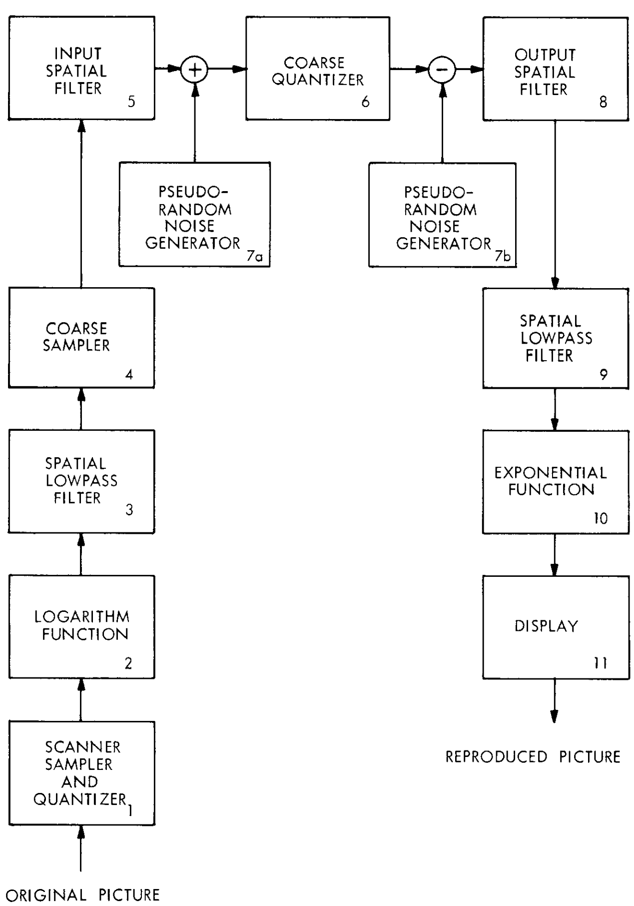

Fig. XI-3. Experimental system.

The goal in the design of the Experimental system was two-fold: first, to examine the feasibility of the proposed comparison system; and second, to combine the results of some previous image-transmission experiments into a novel source coding scheme. An outline of the Experimental system is presented in Fig. XI-3. (All block-number designations in this section refer to Fig. XI-3.)

Blocks 1, 3, 4, 6, 7a, 7b, 9, and 11 are identical in function to the corresponding blocks in the Standard system. The increase in coding efficiency is provided by blocks 2, 5, 8, and 10, which will be described.

The image processing in this system is done on the logarithm of the brightness of each sample value as indicated in block 2. The sensitivity of the eye is not uniform over all brightness levels. In fact, the human visual system responds linearly to multiplicative rather than linear changes in brightness.[4] The use of the logarithm function compensates for this by concentrating any error such as quantizing noise in lighter areas of the picture. Thus the observer perceives the errors as uniformly distributed over the brightness range. This process is known as "companding."[3]

The other major addition in the Experimental system is the prequantization and postquantization spatial filters, blocks 5 and 8 (referred to as the input and the output filters, respectively). The goal here was to remove some of the visible random noise introduced by the Roberts technique. Graham considered[5] the problem of designing linear input and output filters to remove visible quantization noise. He modeled the quantization noise as additive noise independent of the image data and determined filters that minimized the mean-square difference between the final image and the initial one, while taking into consideration the spatial frequency response of human vision. Post approximated[6] Graham's results with a set of filters shown in Fig. XI-4. These were the filters used in blocks 5 and 8. Figure XI-2d demonstrates the performance of the Experimental system. (The parameters N, S, QF, and QC are the same as in Fig. XI-2c.)

The improvement in performance of the Experimental system over the Standard system cannot be adequately judged solely from the example presented here. It is necessary

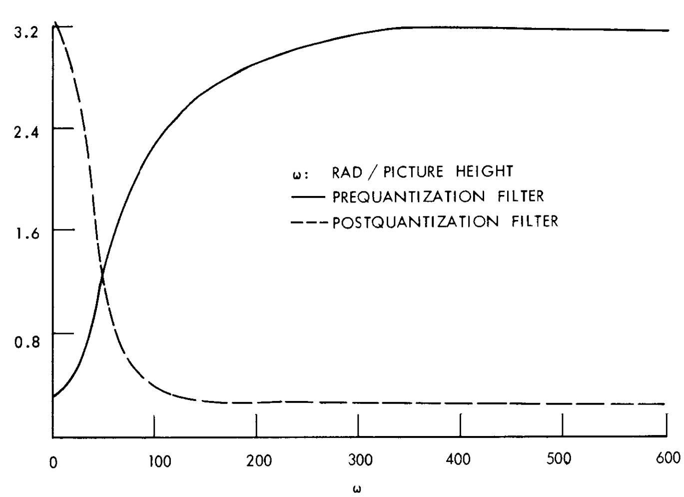

Fig. XI-4. Frequency response of prequantization and postquantization filters.

to consider the change in system performance as the parameters that are involved vary. The goal of the comparison technique, which will be outlined briefly was to account for each factor affecting quality separately until the performance of a system could be described as a function of as few parameters as possible. Considering this, the comparison technique that was used was the following.

1. For a given transmission scheme and capacity C and a particular picture, obtain the qualitatively best reproduction by altering QC (and, of course, S).[7]

2. Assemble two series of results from Part 1 for various values of C: one, using the Standard system; and the other, the Experimental system.

3. Select reproductions of the same quality from each series and compute the compression ratio: C for the Standard picture divided by C for the Experimental picture.

4. The system performance is now noted as the variation of the compression ratio with C for the Standard system and with the subject matter.

In the present research, the three subjects shown in Fig. XI-5 were chosen because they represent typical television or newspaper scenes and also present different ranges of detail. Figure XI-6 shows an example of one of the groups of photographs examined for Part 1 of the test. Twelve observers participated: six were trained (i. e., they have done research in image processing). The choices of the observers for this particular test are tabulated as follows.

Standard System. (Capacity = 16,384 bits).

Observers	QC = 6	QC = 5	QC = 4	QC = 3	QC = 2
Trained	1	1	2	2	0
Untrained	0	4	2	0	0

Figure XI-7 shows an example of the results of Part 4 of the test. Each grouping of X's

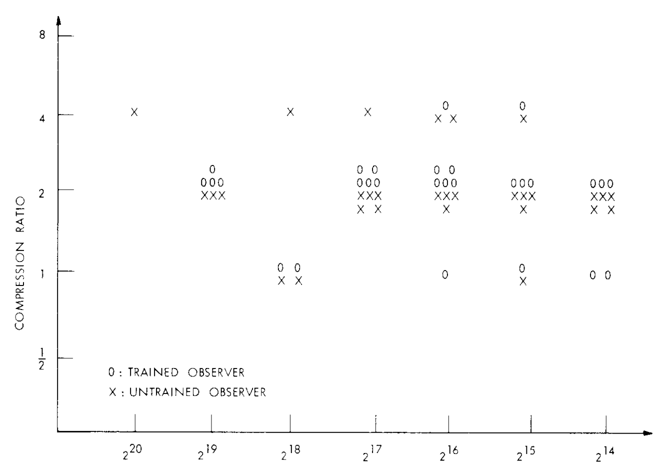

Fig. XI-7. Compression ratio vs channel capacity for the "crowd" picture.

GIRL

CAMERAMAN

CROWD

Fig. XI-5. Original pictures for the comparison tests.

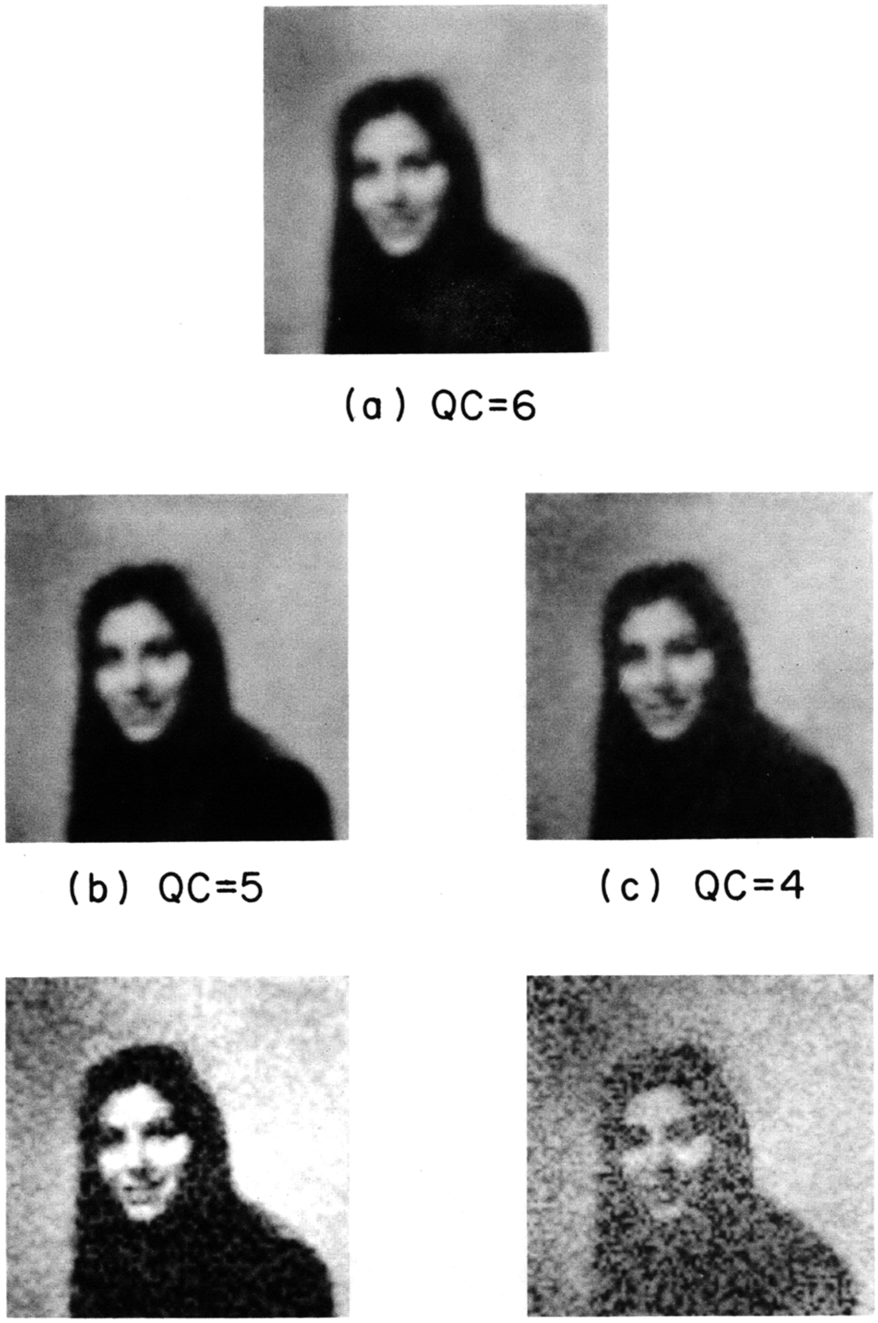

(a) QC=6

(b) QC=5

(c) QC=4

(d) QC=3

(e) QC=2

Fig. XI-6. Example of Part 1 of the comparison tests.

and 0's represent a single compression ratio for a particular capacity for the Standard system. In all three cases the compression ratio averaged approximately two; that is, the Experimental system afforded approximately a 50% saving in bandwidth over the Standard system, for equal subjective quality.

K. P. Wacks

Footnotes and References

1. The reason for using this well-known variant as the "Standard" system rather than straightforward PCM is that it yields superior quality for a given channel capacity. Given the present electronics technology and knowledge of the properties of image-transmission systems, there appears to be little reason for ever building a PCM system that does not use this or similar techniques.

2. D. P. Petersen and D. Middleton, "Sampling and Reconstruction of Wave-Number-Limited Functions in N-Dimensional Euclidean Spaces," Inform. Contr. 5, 279-323 (1962).
3. L. G. Roberts, "Picture Coding Using Pseudo-Random Noise," IRE Trans., Vol. IT-8, No. 2, pp. 145-154, February 1962.
4. R. M. Evans, An Introduction to Color (John Wiley and Sons, Inc., New York, 1948).
5. D. N. Graham, "Two-Dimensional Filtering to Reduce the Effect of Quantizing Noise in Television," S. M. Thesis, Massachusetts Institute of Technology, May 1966.
6. E. A. Post, "Computer Simulation of a Television Quantizing Noise Filtering System," S. B. Thesis, Massachusetts Institute of Technology, May 1966.

7. This technique was proposed by Professor William F. Schreiber.

B. APPROXIMATION OF A MATRIX BY A SUM OF PRODUCTS

1. Introduction

In many cases, such as numerical evaluation of matrix products or two-dimensional convolution, it is useful to approximate a matrix by a small number of terms. We shall explore an approximation of the form

$$A = \sum_{i=1}^{m} x^i y^i_T$$

and present an optimal procedure for obtaining this approximation. If A has a certain type of symmetry, the expansion can be made with fewer terms than might otherwise be required.

2. Notation

Matrices will be represented by upper-case letters, and matrix components by lower-case letters with two subscripts.

$$A = [a_{ij}].$$

The first subscript is a row index, and the second a column index. Exceptions are one-column matrices, which are represented by lower-case letters, and collections of these are indexed by superscripts. Superscript stars indicate complex conjugates. Scalars will be represented by lower-case Greek letters.

3. Approximation Theorem

We seek to approximate a matrix A by an expansion of the form

$$B = \sum_{i=1}^{m} x^i y_T^i.$$

The expansion is to be made so that the error, defined by

$$\epsilon = \sum_{i,j} |a_{ij}-b_{ij}|^2,$$

will be as small as possible. This best approximation is given by the following theorem.

Theorem 1.

Let u^i be the eigenvectors of the equation

$$A_T A^* u^i = \mu_i u^i.$$

A is a $\ell \times n$ matrix. All eigenvalues μ_i are real and non-negative, and we order them according to the rule

$$i > j \Longrightarrow \mu_i \geq \mu_j.$$

Let

$$v^i = A^* u^i.$$

The best m-term approximation to A is given by

$$B = \sum_{i=1}^{m} v^{i*} u_T^i, \tag{1}$$

and the error is given by

$$\epsilon = \sum_{i=m+1}^{\ell} \mu_i. \tag{2}$$

Discussion. The proof makes use of the following theorem (Lanczos[1]).

Let λ_i, u^i, w^i be associated with the characteristic equations

$$A^* u^i = \lambda_i w^i$$

$$A_T w^i = \lambda_i u^i.$$

The eigenvectors are normalized:

$$u^i_T u^{i*} = 1$$

$$w^i_T w^{i*} = 1.$$

All λ_i are real, and A is identical to

$$A = \sum_i \lambda_i w^{i*} u^i. \tag{3}$$

This theorem, which we call the expansion theorem, has the following relation to the approximation theorem.

1. $\mu_i = \lambda_i^2$.

2. u^i is the same in both theorems.

3. $v^i = \lambda_i w^i$.

The following results may also be obtained.

4. $u^i_T u^{j*} = \delta_{ij}$

5. $w^i_T w^{j*} = \delta_{ij}$.

Expansion 1 is not unique. We may, for example, replace v^i with $v^i \alpha_i^*$ and u^i with u^i/α_i, and B will be unchanged. In fact, for any nonsingular matrix X we can calculate

$$Y = A_T X_T^{-1}$$

and then

$$A = XY_T.$$

The columns of X and Y are vectors that are appropriate for an expansion such as in (3). This multiplicity presents a serious difficulty: the error ϵ does not have a unique stationary point, and differential techniques are not very useful.

We use the following procedure in our proof: We shall derive a convenient form for the error, split this into a sum of non-negative terms, and then show that each of these terms has minimum value for the expansion specified in the Theorem 1 statement.

We begin by writing the expansion theorem in a more convenient form. Let A be an $\ell \times n$ matrix, and assume $n \geq \ell$. The characteristic equations may be written

$$A^* U = W\Lambda$$

$$A_T W = U\Lambda$$

U is an $n \times \ell$ matrix whose columns are the u^i, W is an $\ell \times \ell$ matrix whose columns are the w^i, and Λ is an $\ell \times \ell$ diagonal matrix whose elements are the eigenvalues λ_i. We chose W so that $\lambda_i \geq 0$, and the λ are ordered in decreasing magnitude.

$$U_T U^* = I$$

$$W_T W^* = WW_T^* = I$$

$$A = W^* \Lambda U_T \tag{4}$$

$$A_T A^* = U\Lambda^2 U_T^*$$

$$AA_T^* = W^* \Lambda^2 W_T. \tag{5}$$

Armed with this, we proceed to a simple form of the error expression.

Lemma 1

Let

$$c^k = W_T^* x^{k*} \tag{6}$$

$$d^k = U_T^* y^k. \tag{7}$$

Then the error is given by

$$\epsilon = \sum_{i=1}^{\ell} \lambda_i^2 - 2\,\mathrm{Re}\left(\sum_{k=1}^{m} \sum_{i=1}^{\ell} \lambda_i c_i^{k*} d_i^k\right)$$

$$+ \sum_{k=1}^{m} \sum_{j=1}^{m} x^k x_T^{j*} y^k y_T^{j*}. \tag{8}$$

Proof: One may see by evaluation that

$$\sum_{i=1}^{m} \sum_{j=1}^{n} |a_{ij}|^2 = \mathrm{Trace}\left(AA_T^*\right),$$

so that

$$\epsilon = \mathrm{Trace}\left(\left(A - \sum_{k=1}^{m} x^k y_T^k\right)\left(A_T^* - \sum_{k=1}^{m} y^{k*} x_T^{k*}\right)\right).$$

By expanding and substituting (4) and (5), we obtain

$$\epsilon = \mathrm{Trace}\left(W^* \Lambda^2 W_T - W^* \Lambda U_T \sum_{k=1}^{m} y^{k*} x_T^{k*}\right.$$

$$\left. - \sum_{k=1}^{m} x^k y_T^k U^* \Lambda W_T\right)$$

$$+ \sum_{i=1}^{m} \sum_{k=1}^{m} \left(y_T^i y^{k*}\right)\left(x_T^i x^{k*}\right).$$

Since trace is invariant under a unitary transformation, this is identical to

$$\epsilon = \mathrm{Trace}\,(\Lambda^2) - \mathrm{Trace}\left(\Lambda \sum_{k=1}^{n} U_T y^{k*} x_T^{k*} W^*\right)$$

$$- \mathrm{Trace}\left(\sum_{k=1}^{n} W_T x^k y_T^k U^* \Lambda\right)$$

$$+ \sum_{i=1}^{m} \sum_{k=1}^{m} \left(y_T^i y^{k*}\right)\left(x_T^i x^{k*}\right).$$

Substituting (6) and (7) and evaluating the trace produces (8).

Q. E. D.

We shall now show that the vectors x_i and y_i may be required to be orthogonal.

Lemma 2.

Any matrix given by

$$M = \sum_{k=1}^{m} x^k y_T^k$$

can be written

$$M = \sum_{k=1}^{m} \mu_k g^k h_T^k,$$

where

$$g_T^k g^{\ell *} = \delta_{k\ell}$$

$$h_T^k h^{\ell *} = \delta_{k\ell}$$

$$\mu_k \sim \text{real.}$$

Proof:

$$m_{ij} = \sum_{k=1}^{m} g_i^k h_j^k.$$

consider

$$Mx = \sum_j \sum_k g_i^k h_j^k x_j = \sum_{k=1}^{m} g^k \left(h_T^k x\right),$$

so that the image of Mx is at most m-dimensional. A similar result can be obtained for $M_T x$. Therefore MM_T and $M_T M$ can have at most m nonzero eigenvalues, and an expansion such as that given in (3) will contain at most m terms.

Q. E. D.

Proof of Theorem 1. Using Lemma 2, we expand B:

$$x^k = \mu_k g^k$$

$$y^k = h^k$$

$$e^k = W_T^* g^{k*} \qquad c^k = \mu_k e^k$$

$$d^k = U_T^* h^k$$

$$\left(g^k g_T^{\ell *}\right) = \delta_{k\ell}$$

$$\left(h^k h_T^{\ell *}\right) = \delta_{k\ell}$$

the error becomes

$$\epsilon = \sum_{i=1}^{\ell} \lambda_i^2 - 2 \operatorname{Re} \left(\sum_{i=1}^{\ell} \sum_{k=1}^{m} \mu_k \lambda_i e_i^{k*} d_i^k \right) + \sum_{k=1}^{m} \mu_k^2.$$

This function is quadratic in μ_k and the minimum occurs for

$$\mu_k = \sum_{i=1}^{\ell} \lambda_i \operatorname{Re} \left(e_i^{k*} d_i^k \right).$$

Therefore

$$\epsilon \geqslant \sum_{i=1}^{\ell} \lambda_i^2 - \sum_{k=1}^{m} \left(\sum_{i=1}^{\ell} \lambda_i \operatorname{Re} \left(e_i^{k*} d_i^k \right) \right)^2 .$$

We now apply the Schwartz inequality. Since $\lambda_i \geqslant 0$,

$$\left(\sum_{i=1}^{\ell} \lambda_i \operatorname{Re} \left(e_i^{k*} d_i^k \right) \right)^2 = \left(\operatorname{Re} \left(\sum_{i=1}^{\ell} \left(e_i^{k*} d_i^k \right) \right) \right)^2$$

$$\leqslant \left| \sum_{i=1}^{\ell} \lambda_i e_i^{k*} d_i^k \right|^2 \leqslant \left(\sum_{i=1}^{\ell} \lambda_i \left| e_i^k \right|^2 \right) \left(\sum_{i=1}^{\ell} \lambda_i \left| d_i^k \right|^2 \right),$$

and

$$\epsilon \geqslant \sum_{i=1}^{\ell} (\lambda_i)^2 - f, \tag{9}$$

with

$$f = \sum_{k=1}^{m} \left(\sum_{i=1}^{\ell} \lambda_i |e_i^k|^2 \right) \left(\sum_{i=1}^{\ell} \lambda_i |d_j^k|^2 \right). \tag{10}$$

We now compute a test value of the error. The set

$$x^k_{Test} = \mu_k w^k$$

$$y^k_{Test} = u^k$$

produces

$$e_i^k = \delta_{ki} \tag{11}$$

$$d_i^k = \delta_{ki}, \tag{12}$$

and

$$\epsilon_{Test} = \sum_{k=m+1}^{\ell} \lambda_k^2. \tag{13}$$

Equation 9 takes on the same value. Let us consider a component term in (10). The relation

$$\sum_{i=1}^{\ell} \lambda_i |e_i^k|^2 = \sum_{i=1}^{\ell} (\lambda_i - \lambda_{i+1}) \sum_{o=1}^{i} |e_o^k|^2$$

may be proved by induction on ℓ. For notational convenience, we assume that $\lambda_{\ell+1} = 0$. In terms of this expansion, f becomes

$$f = \sum_{i=1}^{\ell} \sum_{j=1}^{\ell} (\lambda_i - \lambda_{i+1})(\lambda_j - \lambda_{j+1}) \sum_{k=1}^{m}$$
$$\cdot \left(\sum_{o=1}^{i} |e_o^k|^2 \right) \left(\sum_{p=i}^{i} |d_p^k|^2 \right).$$

If we substitute the test values of e^k, d^k from (11) and (12), we obtain

$$f_{Test} = \sum_{i=1}^{\ell} \sum_{j=1}^{\ell} (\lambda_i - \lambda_{i+1})(\lambda_j - \lambda_{j+1})\, h_{ijm},$$

with

$h_{ijm} = \min(i, j, m).$

Consider

$$\ell_{ijm} = \sum_{k=1}^{m} \sum_{o=1}^{i} \sum_{p=1}^{j} |e_o^k|^2 |d_p^k|^2.$$

We establish the following inequalities.

$$\sum_{p=1}^{i} |d_p^k|^2 \leq 1 \tag{14}$$

$$\sum_{o=1}^{i} |e_o^k|^2 \leq 1 \tag{15}$$

$$\sum_{k=1}^{m} |d_p^k|^2 \leq 1 \tag{16}$$

$$\sum_{k=1}^{m} |e_o^k|^2 \leq 1. \tag{17}$$

Since the columns of U are orthonormal, we may form an $(n \times n)$ unitary matrix P by augmenting U.

$$P = [U \mid S]$$

$$PP_T^* = I = P_T P^*.$$

We define d^{1k} by

$$d^{1k} = P_T^* h^k.$$

Note that

$$d_p^{1k} = d_p^k \qquad \text{for} \quad p \leq \ell, \ k \leq m.$$

So that we prove (14) by

$$\sum_{p=1}^{i} |d_p^k|^2 \leq d_p^{1k} d^{1k*} = h_T^k P^* P_T h^{k*}$$

$$= h_T^k h^k = 1.$$

Equation 15 is proved in a similar way.

We now note that

$$d_T^{1k} d^{1\ell *} = h_T^k P^* P_T h^{\ell *}$$

$$= h_T^k h^{\ell *} = \delta_{k\ell}.$$

So that we may form a unitary matrix D whose first m columns are the d^{1k}.

$$d_{pk} = d_p^k \qquad k \leqslant m$$
$$p \leqslant \ell.$$

Since this matrix is unitary,

$$\sum_{k=1}^{n} d_{pk} d^*_{pk} = 1 \geqslant \sum_{k=1}^{m} |d_p^k|^2$$

which proves (16). Equation 17 is proved in a similar way.

Consider ℓ_{ijm}. By applying (14), we get

$$\ell_{ijm} = \sum_{k=1}^{m} \sum_{o=1}^{i} \sum_{p=1}^{j} |e_o^k|^2 |d_p^k|^2$$

$$\leqslant \sum_{k=1}^{m} \sum_{o=1}^{i} |e_o^k|^2. \tag{18}$$

Similarly,

$$\ell_{ijm} \leqslant \sum_{k=1}^{m} \sum_{p=1}^{i} |d_p^k|^2 \tag{19}$$

If we apply (15) to (18), we obtain

$$\ell_{ijm} \leqslant \sum_{k=1}^{m} 1 = m. \tag{20}$$

And if we apply (17) to (18), we get

$$\ell_{ijm} \leqslant \sum_{o=1}^{i} 1 = i \tag{21}$$

Finally, by applying (16) to (19), we obtain

$$\ell_{ijm} \leqslant \sum_{o=1}^{i} 1 = j. \tag{22}$$

By combining (20), (21), and (22),

$$\ell_{ijm} \leqslant \min\ (i,j,m) = h_{ijm}.$$

Since from our ordering $(\lambda_i-\lambda_{i+1})$ is greater than zero, f is a sum of non-negative terms, each of which is bounded by $(\lambda_i-\lambda_{i+1})(\lambda_j-\lambda_{j+1})\ h_{ijk}$, so that

$$f \leqslant f_{Test},$$

and

$$\epsilon \geqslant \sum_{k=1}^{\ell} \lambda_k^2 - f_{Test}.$$

This value of ϵ is achieved by the set of vectors proposed in the statement of the theorem.

Q. E. D.

4. Symmetry Considerations

The number of terms required to represent matrix A exactly is equal to the number of nonzero characteristic values of the matrix AA_T^*. If A is an $\ell \times n$ matrix, it will have at most

$$r = \min\ (\ell, n)$$

nonzero eigenvalues. Under some circumstances, the number of nonzero eigenvalues is smaller: in particular, this happens if A has a certain kind of symmetry. If for example, $a_{ij} = a_{\ell+1-i,j}$ and $a_{i,j} = a_{i,n+1-j}$, then only approximately r/2 eigenvalues of the matrix are nonzero.

To talk about this sort of symmetry, we shall define an $\ell \times \ell$ matrix F by the formula

$$f_{ij} = \begin{cases} 1 & \text{if } i+j = \ell+1 \\ 0 & \text{otherwise.} \end{cases}$$

Note that $F^2 = I$. If we premultiply by this matrix, the rows are interchanged last with first, second with next-to-last, etc. Postmultiplication by this matrix interchanges the columns in the same way.

Theorem 2.

Let C be an $r \times r$ matrix such that

$$C_T = C^*$$

$$CF = C.$$

Then C will have at most s nonzero eigenvalues,

$$s = [(r+1)/2],$$

where $[a]$ represents the integral part of a.

Proof of Theorem 2: The hypothesis above implies that FC = C because

$$FC = (C^* F)_T = (CF)_T^* = C_T^* = C.$$

If x is an eigenvector with λ eigenvalue, then Fx will be an eigenvector of the same eigenvalue because

$$C(Fx) = (CF)x = Cx = (FC)x = F(cx) = \lambda(Fx).$$

Consider x - Fx. This will be also an eigenvector with the same eigenvalue, yet

$$C(x-Fx) = \lambda(x-Fx) = (C-CF)x = (C-C)x = 0.$$

so that either Fx = x or $\lambda = 0$.

Now consider the set of eigenvectors with nonzero eigenvalues. Since Fx = x, only the first s coefficients of x are independent, so that the subspace spanned by them has only s dimensions. But since all eigenvectors are linearly independent, there may be at most s such vectors.

Corollary. Let A be an $\ell \times n$ matrix, and m the number of terms required to represent it exactly.

Then

1. If FA = A,
   $m \leq [(\ell+1)/2]$.
2. If AF = A,
   $m \leq [(n+1)/2]$.
3. If both 1 and 2 hold, then
   $m \leq [(\min(\ell, n)+1)/2]$.

Proof: This follows by applying Theorem 2 to either AA_T^* or $A_T A^*$,

O. J. Tretiak

References

1. C. Lanczos, Linear Differential Operators (D. Van Nostrand, Company, London, 1961), p. 121.

C. FOCUSED ULTRASONIC TRANSDUCER DESIGN

1. Introduction

The usefulness of ultrasonics as a diagnostic medical tool is now an established fact. This introduces a series of problems ranging from the transducers themselves to the form of display that remains to be worked on. In particular, there are spatial resolution limitations imposed by the design of the transducer.

The resolution in distance is determined primarily by the length of the transmitted ultrasonic pulse. The distance is determined by the time required for the pulse to reach the target and return. Thus, at best, the resolution is

$$R_{m/n} = \frac{1\tau}{2C}, \tag{1}$$

where τ is the pulse length, and C is the velocity of propagation.

Asmith resolution, on the other hand, is entirely a function of the beamwidth of the transducer. It is therefore desirable to have as narrow a beam as possible. At a given distance it is possible to have as narrow a beamwidth as desired, limited only by diffraction. In typical applications, however, the targets range over some finite interval; therefore, ideally one would like to design a transducer to produce a narrow beam over that finite interval. This always implies some kind of a compromise lens design, which has been investigated by Kossoff.[1]

Any attempt to lengthen the ringed transducer evaluation focal area will in general,

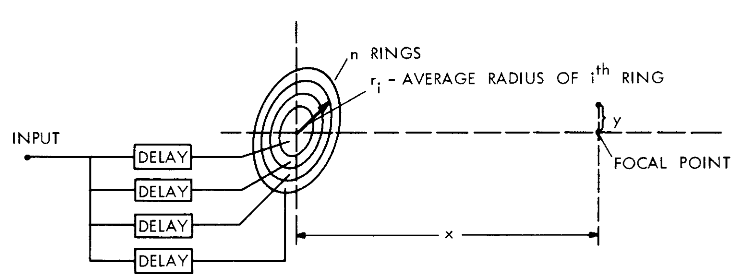

Fig. XI-8. Ringed transducer configuration. n rings, each of average radius, r_i, are driven from a common source through separate delays to place the focal point a distance x from the transducer.

increase the beamwidth. This limitation can in a sense be overcome by working with, instead of against, the properties of the transducers. Specifically, instead of trying to compromise on one lens design, simply make a transducer with an electrically variable focal point. Thus it would be possible to have the focal point track the area that corresponds to the time delay between transmitted and received pulses. Such a transducer is shown in Fig. XI-8.

The transducer is focused by adjusting the delay for each ring so that the total delay between the electrical source and the focal point is the same for all rings.

The delay d_i for the i^{th} ring is

$$d_i = \frac{1}{C}\left(\sqrt{x^2 + r_n^2} - \sqrt{x^2 + r_i^2}\right). \tag{2}$$

To investigate the nature of the field around the focal point would require the evaluation of

$$P = \sum_{i=1}^{n} \int_{r_i^a}^{r_i^b} \int_0^{2\pi} \frac{r\, e^{\frac{2\pi}{\lambda}\sqrt{x^2 + (r-y)^2 \cos^2\theta + r^2 \sin^2\theta}}}{\sqrt{x^2 + (r-y)^2 \cos^2\theta + r^2 \sin^2\theta}}\, d\theta dr, \tag{3}$$

where r_i^a and r_i^b are the inner and outer radii, respectively of the i^{th} ring. This integral cannot in general be evaluated in closed form. Thus, a Taylor series expansion was made

$$r_i^o = \frac{1}{2}\left(r_i^a + r_i^b\right) \tag{4}$$

$$\begin{aligned} A_i(r,\theta) &= \sqrt{x^2 + r_i^{o2} + y^2} + \left(r - r_i^o\right) \frac{\partial}{\partial r}\left(\sqrt{x^2 + (r-y)^2 \cos^2\theta + r^2 \sin^2\theta}\right) \\ &\quad + \cos\theta \frac{\partial}{\partial \cos\theta}\left(\sqrt{x^2 + (r-y)^2 \cos^2\theta + r^2 \sin^2\theta}\right) \\ &= \sqrt{x^2 + r_i^{o2} + y^2} + \frac{\left(r - r_i^o\right)\left(r_i^o - y\cos\theta\right) - ry\cos\theta}{\sqrt{x^2 + r_i^{o2} + y^2}}. \end{aligned} \tag{5}$$

By also assuming that $A(r,\theta)$ varies slowly from r_i^a to r_i^b, the integral can be approximated by

$$P = \sum_{i=1}^{n} \int_{r_i^a}^{r_i^b} \frac{r}{\sqrt{x^2 + r_i^{o2} + y^2}} \int_0^{2\pi} e^{\frac{j2\pi}{\lambda} A_i(r,\theta)}. \tag{6}$$

Let

$$Z_i = \sqrt{x^2 + r_i^{02} + y^2}. \tag{7}$$

Then

$$P = \sum_{i=1}^{n} \frac{e^{\frac{j2\pi}{\lambda}\left(Z_i - \frac{r_o^2}{Z_i}\right)}}{Z_i} \int_{r_i^a}^{r_i^b} r\, e^{\frac{j2\pi}{\lambda}\left(\frac{r-r_i^o}{Z_i}\right)} J_o\left(\frac{2\pi}{\lambda}\, \frac{\left(2r-r_i^o\right) y}{Z_i}\right). \tag{8}$$

This definite integral can then be evaluated on a computer by a power-series expansion of the integrand.

2. Ring Configuration

The simplest possible ring configuration would be circular rings of equal width. This leads to a severe limitation on the lower number of rings that can be used. The source of the limitation is shown in Fig. XI-9. When the distance w_i becomes a significant part

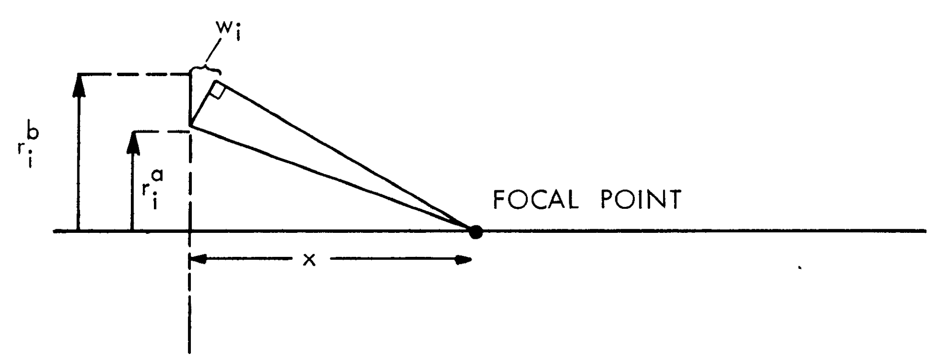

Fig. XI-9. Ring width limitation. The distance $w_i \approx \left(r_i^b - r_i^a\right) \frac{r_i^a}{x}$ limits the maximum width of a single ring.

of a wavelength, then the ring is not contributing all of its output energy to the area around the focal point.

To some extent, it is possible to get around this limitation by using nonuniform ring widths. Since w increases with both $1/2\left(r_i^a+r_i^b\right)$ and $\left(r_i^b-r_i^a\right)$, it would be reasonable to increase $\left(r_i^b-r_i^a\right)$ as $1/2\left(r_i^a+r_i^b\right)$ decreases. In particular, to make w uniform on all rings a Fresnel-line ring pattern can be used, which gives

$$\frac{\sqrt{r_n^2+x^2}-x}{n}=\sqrt{r_i^{b2}+x^2}-\sqrt{r_i^{a2}+x^2} \qquad i=1,2,\ldots n. \tag{9}$$

It would appear that this ring configuration would be a function of the focal distance x. While this is true in an analytical sense, in practice the ring widths vary slowly with varying x. Thus they can be chosen for a value of x in the center of the range to be covered.

3. Array Approach

Another class of electrically controlled transducers is the steerable array. Normally such an array is composed of a grid of elements excited in such a manner as to produce the same delay between all adjacent elements in the plane of the desired beam.

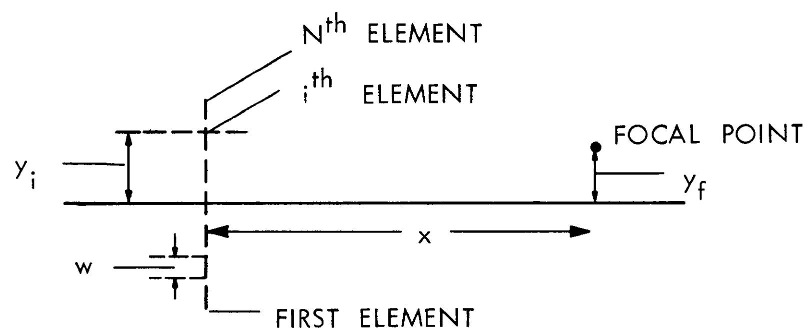

Fig. XI-10. Array transducer configuration. n elements, each of width w, at a distance y_i from the axis are focused to a point y_f from the axis and a point x from the transducer.

Such a system would have a focus at infinity. To move the focus to the range of interest to medical applications requires that the delay introduced in each element plus the acoustical delay from the element to the focal point be constant. Thus the delay for the ith element is

$$d_i=\max_{1\leqslant j\leqslant n}\left(\sqrt{x^2+(y_j-y_f)^2}-\sqrt{x^2+(y_i-y_f)^2}\right), \tag{10}$$

where d_i is the delay, and x, y_i, y_f are as indicated in Fig. XI-10.

To obtain the exact value of the field at the focal point requires evaluation of

$$P = \sum_{i=1}^{N} \int_{y_i-w/2}^{y_i+w/2} e^{j\frac{2\pi}{\lambda}\left[\sqrt{x^2+(r-y_f)^2}-d_i\right]} dr$$

which can be approximated by a Taylor series expansion of the radical to give

$$P = \sum_{i=1}^{N} e^{j\frac{2\pi}{\lambda}\left(\sqrt{x^2+(y_i-y_f)^2}-d_i\right)} \int_{y_i-w/2}^{y_i+w/2} e^{j\frac{2\pi}{\lambda}\left[\frac{(r-y_i)(y_i-y_f)}{\sqrt{x^2+(y_i-y_f)^2}}\right]} dr. \tag{11}$$

Equation 11 can then be evaluated directly.

4. Calculated Results

Computer programs were written to evaluate Eqs. 8 and 11. The ring transducer program using (8) was run for transducers, 26, 40, and 60 mm in diameter,

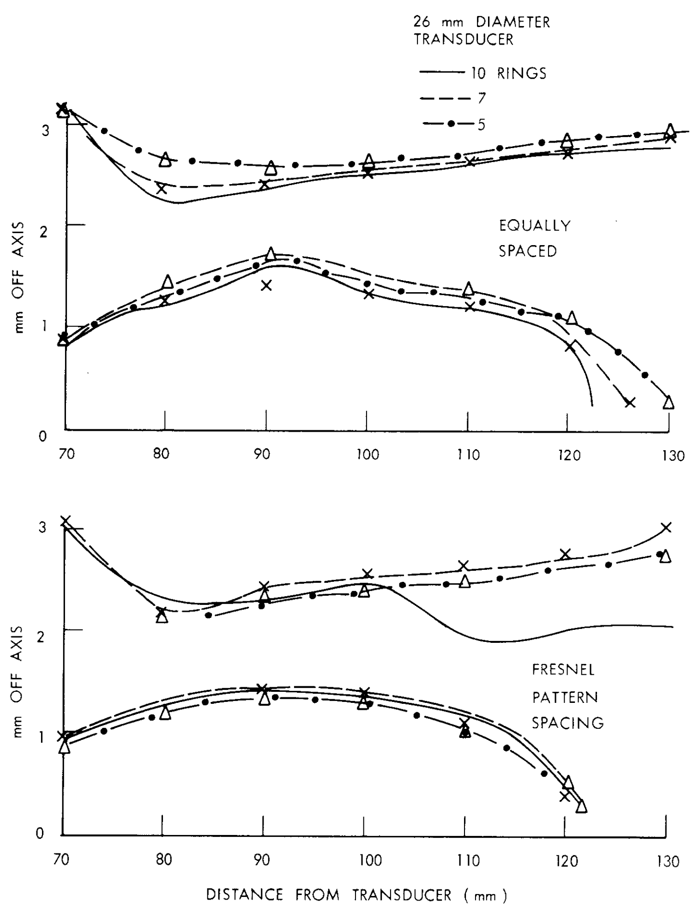

Fig. XI-11. Field of a transducer, 26 mm in diameter, focused 100 mm away.

with from 5 to 15 rings, and for a wavelength of 0.75 mm. Both equal spacing and Fresnel pattern spacing were used. In all cases the focal point was set at 100 mm from the transducer.

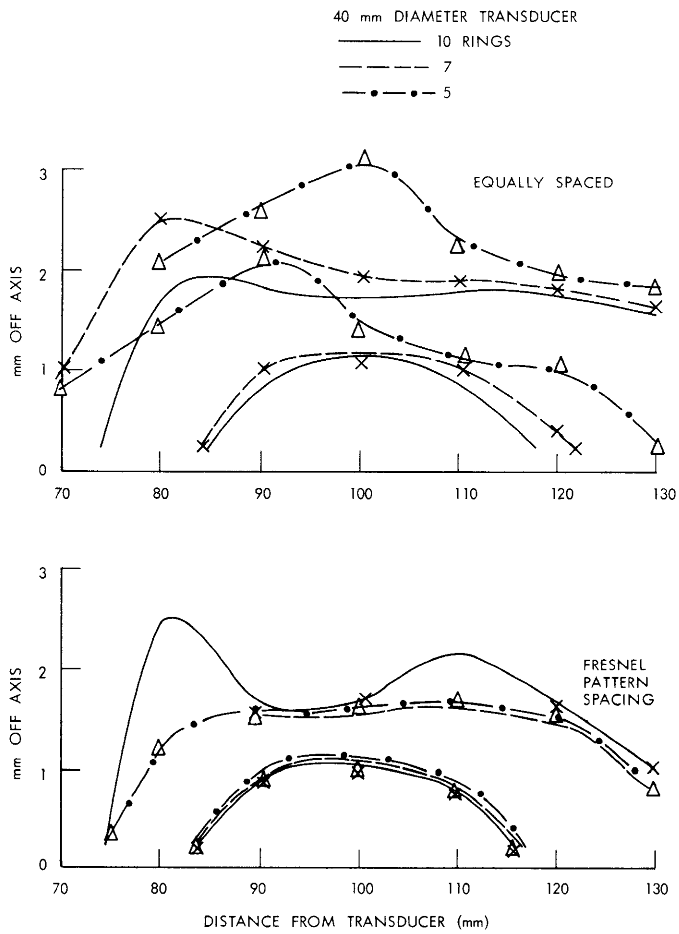

Fig. XI-12. Field of a transducer, 40 mm in diameter, focused 100 mm away.

The results of these computations are shown in Figs. XI-11, XI-12, and XI-13. As can be seen in all figures, the use of the Fresnel pattern design leads to a smaller area within the -3 dB and -10 dB contours for a given number of rings.

The peak value of the error in the approximation was also calculated by evaluating

$$e = \max_{0\leq y\leq y_{max}} \max_{1\leq i\leq N} \max_{0\leq\phi\leq 2\pi} \max_{r_i^a\leq r\leq r_i^b} \left| \sqrt{x^2+(r-y)^2\cos^2\theta+r^2\sin^2\theta} - A_i(r,\phi) \right|.$$

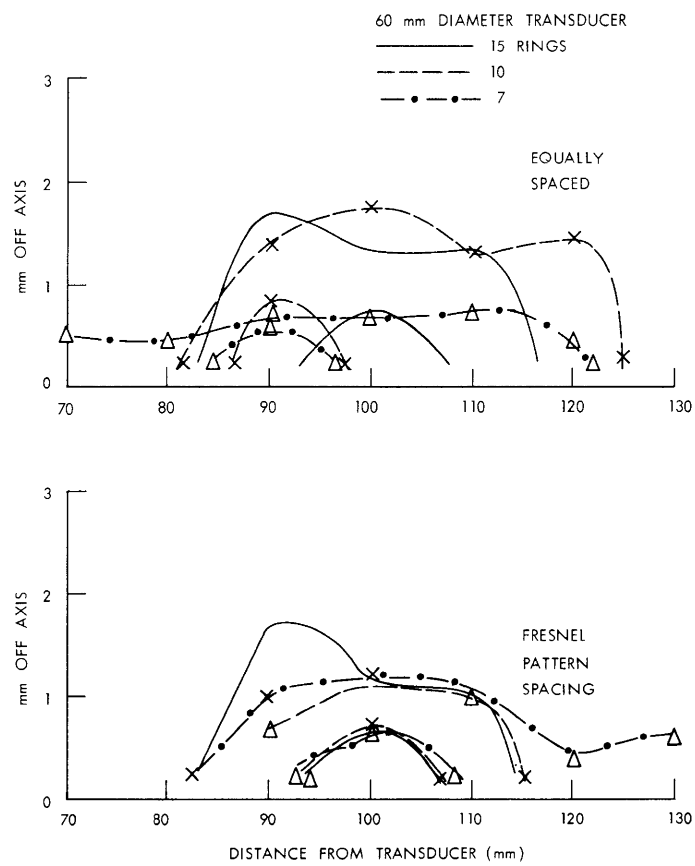

Fig. XI-13. Field of a transducer, 60 mm in diameter, focused 100 mm away.

This value is shown in Table XI-1.

Since at worst e increases in a linear fashion with $\left(r-r_i^o\right)$, and the value of e shown occurs for only one ring, a conservative estimate for the rms value of the error would be

$$e\sqrt{\frac{1}{\int_0^1 x\,dx}} = \frac{e}{\sqrt{2}},$$

which is less than 1/8 of a wavelength for most of the cases.

The program using (11) for the array design was run for an array, 100 mm long, with 20, 30, 50, 75, and 100 elements, from .75 to 1.5 mm wide, and at a wavelength of 0.75 mm.

Table XI-1. Peak error in the approximation.

Number of Rings	Diameter (mm)	Error with Equal Spacing (mm)	Error with Fresnel Pattern Spacing (mm)
5	26	.05	.12
7	26	.02	.12
10	26	.01	.02
5	40	.07	.17
7	40	.06	.13
10	40	.03	.13
7	60	.04	.21
10	60	.04	.15
15	60	.02	.13

Since such a design leads to a very small focal area, the distance to the first side lobes and their amplitude were tabulated in Table XI-2.

Table XI-2. Side lobes resulting from an array transducer.

Number of Elements	Element Width (mm)	Distance from Focal Point to First Side Lobe (mm)	Amplitude of First Side Lobe with Respect to Amplitude at Focal Point (dB)
20	3	15	+2.5
20	1.5	15	−5
20	.75	15	−7.7
30	1.5	23	−2.2
30	.75	23	−5
50	1.5	38	−10.3
50	.75	38	−12.2
75	1.0	>67*	–
100	.75	>100*	–

*Exceeded limits imposed by the program.

5. Conclusions

The use of transducers with an electrically movable focal point appears to be practical. It has been shown that a transducer only 26 mm in diameter with just 5 rings could give a focal area 2.5 mm in radius at the −10 dB contour. Such a transducer and its associated electronics equipment would not be an unreasonable system to implement.

Although the results look favorable for both the ring and array type of transducer, one additional factor must be accounted for. That is the inheterogeneous nature of the tissue that this system would actually be used to image. Therefore, the next stage in this investigation will be to attempt to account for this. This will be done by introducing a random amount of delay into each of the elements or rings. To determine the statistics of the required random variable, preparations are now being made to measure the acoustic properties of tissue in the cat brain and skull. We expect that these measurements will be completed by September 1970, at which time a transducer will be designed and evaluated with the techniques described here, and finally, a complete system will be constructed.

M. Hubelbank, O. J. Tretiak

References

1. G. Kossoff, Report of Commonwealth Acoustic Laboratories No. 17, Australia Department of Health, May 1962.

D. TACTILE PITCH FEEDBACK FOR THE PROFOUNDLY DEAF

Deaf speakers are known to have higher fundamental frequencies than normal-hearing speakers and to have poor control of the inflections and intonations that make speech sound natural and convey meaning.

Researchers have devised visual pitch displays to use as teaching aids for deaf speakers. The deaf have been made aware that voice pitch is important and that their control of pitch is poor. Improvements in intelligibility and pleasantness have resulted for deaf speech.

Little work has been done, however, to use the tactile sense as a partial substitute for hearing. In particular, no work has been done with tactile pitch displays. Since displays might be located anywhere on the body and not require use of a deaf person's eyes, they offer a potential for continuous feedback with no reduction in lipreading ability. Under the direction of Professor Francis F. Lee, a study has been undertaken to investigate the feasibility of tactile feedback as a speech aid for the profoundly deaf.

A pitch detector and simple tactile display have been constructed. The detector processes a throat microphone wave by counting zero crossings at the fundamental frequency; the range of pitch frequencies is quantized into 8 bands, and the number of counts in each band is recorded. The tactile display uses either two or three solenoid pokers. Any band can be assigned to any poker, so that "high" and "low," or "high," "low," and "ok" bands can be determined as appropriate for each deaf speaker.

Experiments were conducted with 26 students at the Boston School For the Deaf. All had suffered sensorineural hearing loss, most of them since birth. The subjects were in the 13-17 year age group and were evenly divided between male and female. The immediate effectiveness of tactile pitch feedback was tested; no attempt was made to evaluate the benefits of sustained use of the system.

Two sets of experiments were undertaken. The first was to determine the limits of motor control of pitch with tactile feedback and the dependence of performance on the periodic display rate. These tests involved having the deaf speaker hum in a prescribed channel at varying display rates and evaluating the resultant mean-squared error. Preliminary analysis of the data indicates that performance was not very sensitive to display rate when the deaf speaker was asker to hum in a frequency region that was comfortable for him, but excursions from his habitual pitch demanded higher feedback rates for success, and for excursions that were too far no amount of feedback would correct the pitch level. These experiments involving only humming were designed to avoid any linguistic effect on pitch and explore the pitch control system of the deaf in terms of a closed-loop motor system.

The second set of experiments was designed to test the use of tactile feedback as an aid to a deaf speaker engaged in spoken conversation. In general, it involved having the subject utter some standardized phrases while using the tactile display to help himself keep below an upper limit on fundamental frequency. A general trend was noticed in the pitch of the deaf, as it depended on the type of utterance: the mean fundamental frequency increased when the speaker moved from simple humming at a comfortable frequency, to repeating familiar words such as his name, to reading text passages. It appeared that the deaf speakers tried to increase their information rate from kinesthetic feedback by increasing the tenseness of their vocal cords and increasing their vocal effort, to match the increasing information content of their utterances. Furthermore, most subjects practiced an unnatural intonation when voicing, beginning their breath groups at a high pitch, then descending quickly to a more natural tone, as if to increase their ability to detect the onset of voicing. Binary tactile displays seem well-suited to providing an alternative source of feedback regarding onset of voicing and initial pitch level, and preliminary results indicate that the solenoid display that was used did in fact correct the unnaturally high pitch and unnatural intonation pattern in many of the subjects. Results regarding the sensitivity to display rates were similar to those in the humming experiments: high rates became necessary as the control task became more difficult, until finally the tasks became so difficult that no motor control was attempted by the subjects and the feedback parameters became immaterial.

Tactile pitch feedback appears to be a promising approach for improving the quality of deaf speech. Straightforward hardware and uncomplicated displays were adequate to help deaf speakers correct common intonation problems. It now appears reasonable for research to continue on the design of a wearable pitch detector and associated display so as to realize the expected benefits of continuous selfmonitoring.

The final report on this work will be embodied in the author's Master's thesis, which is to be submitted to the Department of Electrical Engineering, M. I. T., in September 1970.

T. R. Willemain

E. OPERATOR INTERACTIVE COMPUTER PROGRAMS FOR ANALYZING BIOLOGICAL TISSUE SECTIONS

For several years, members of our group have worked on the computer analysis of various types of biological smears (Papanicolaou smears, blood smears, and so forth). Recently, we have begun to extend the various image-processing techniques to handle

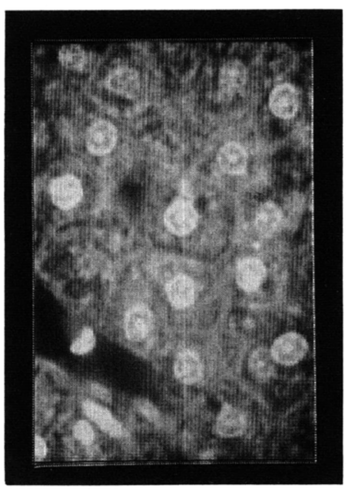

Fig. XI-14.
Photomicrograph of a 7-μ section of liver tissue (500X).

biological tissue sections (see Fig. XI-14). At the outset it was decided that the first step in this work should be to develop a facility for extracting and displaying data from such images so as to give insight into the problems that would be involved in analyzing them. As a result of this decision, a large set of operator interactive routines has been developed to extract information from images and perform various operations on the data. This report will describe these programs and illustrate some of their capabilities.

1. Equipment and Approach

The image-processing work is being done on a DEC PDP-9 computer with a 32k memory and million word disc. The peripherals that are being used in conjunction with the processing are: a high resolution flying spot scanner for scanning transparencies, a photodisplay for making Polaroid prints of pictures, a teletype, a line printer, a cathode-ray tube display, a tablet and pen interfaced with the display for inputting position information, and a calcomp plotter.

The program comprises a set of subroutines for inputting, outputting, and processing information, and a interactive control program that allows the operator to perform the various possible operations in whatever sequence he pleases. The subroutines are written in FORTRAN IV nad MACRO-9, the assembly language for the PDP-9 computer, and the control program is written in FORTRAN IV.

The interaction with the user is via the teletype, the CRT, and the tablet. The approach is to display on the CRT the various possibilities available to the operator at each step in the processing. The operator selects the desired operation via the teletype. Furthermore, at any time when options are being displayed, the operator can

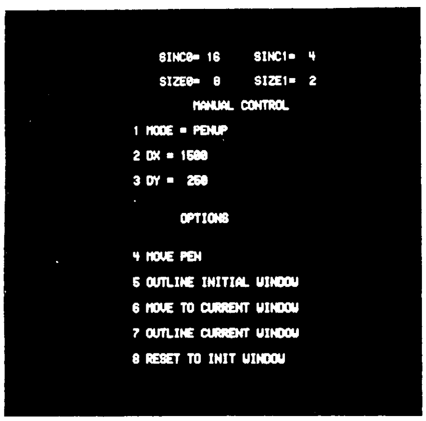

Fig. XI-15.
Typical display of present options available to a user. (This section refers to the calcomp.)

branch to other sections of the program, display or change any of the 200 control parameters in the program, or input or output information to the disc. This is done by using various control characters on the teletype. One of the 20 option displays is shown in Fig. XI-15.

2. Program Description

(a) Initial Scanning and Display

The system is initialized to scan 35-mm transparancies at a raster size of 126 × 186 points with 64 grey levels. The picture is packed into core using 3 points per word, and can be written on disc for future reference. The initial picture is then displayed on the CRT so that the operator can indicate the region of the picture in which he is interested.

(b) Tablet Interaction

The interaction of the user via the tablet is of two sorts: selecting brightness levels for displaying, and defining location information on the picture. Clip levels are selected

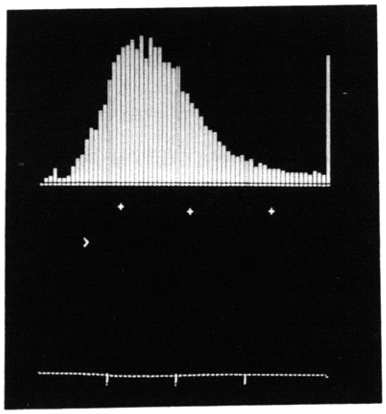

Fig. XI-16.

Histogram of picture shown in Fig. XI-14. The horizontal axis corresponds to brightness (0-63). The vertical axis indicates the relative number of points at indicated brightness.

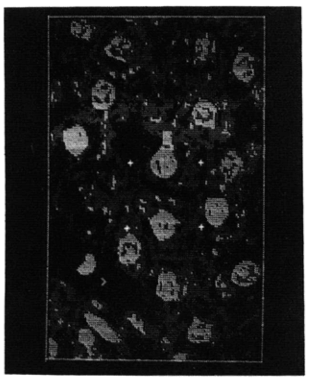

Fig. XI-17.

4-level display of Fig. XI-14. Crosses indicate the region of interest.

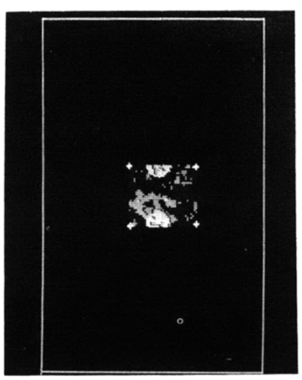

Fig. XI-18.

Display of the region defined in Fig. XI-17.

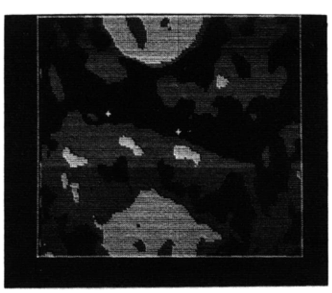

Fig. XI-19.

Same region as in Fig. XI-17, but with 16 times as many points per unit area. The crosses define a vector (pointing to the right).

by allowing the user to input the desired clip levels through the tablet while the picture brightness level histogram is being displayed on the CRT. When the picture is displayed on the CRT, 4 brightness levels are available, and hence the operator selects 3 clip levels. Figure XI-16 shows the histogram for the picture shown in Fig. XI-14. The current display clip levels are indicated by the marks on the baseline. The desired new levels that have been input through the tablet are indicated by the crosses. The current location of the pen is indicated by the cursor.

While the picture is being displayed, the user can use the tablet to define a vector on the picture or to define a rectangular region. The use of the vector will be described in the calcomp section. In the case of the rectangular box, a table is built which describes the section of the picture that is desired; and the various processing programs look at this table in performing their functions. Figure XI-17 shows a display of the slide shown in Fig. XI-14, with 4 brightness levels used. The crosses indicate the desired rectangular region, and Fig. XI-18 shows the corresponding selected region.

(c) Rescanning and Display

In order to look at finer detail in a region of the picture, a region selected as we have described it can be rescanned at a higher scan density. Figure XI-19 shows the same region as Fig. 5 with a 16 times greater scan density.

(d) Printing

The entire picture or any desired section of it can be printed. The operator has the option of printing either the numerical brightness value (0-64) of the points, or symbolic characters chosen to have a darkness in proportion to the brightness of the picture points. At present, 14 such levels are used, and the corresponding clip levels can be chosen either through the tablet or through the teletype.

(e) Displaying and Drawing Contours

Since relative brightness levels of various objects in the picture are usually important, routines have been implemented to search predefined segments of the picture for points either higher or lower than a specified threshold, then follow contours in the image so that points brighter than the threshold are on one side of the contour and points less than or equal to the threshold on the other side. The contours found by these programs can then either be displayed on the oscilloscope or drawn by the calcomp. Figure XI-20 shows such a plot for the bright regions of Fig. XI-14.

(f) Perspective Drawings

One of the main problems in analyzing many types of natural images is that of locating object boundaries, hence routines have been written to give a perspective plot of the brightness along contours in a given direction in any desired region of the picture.

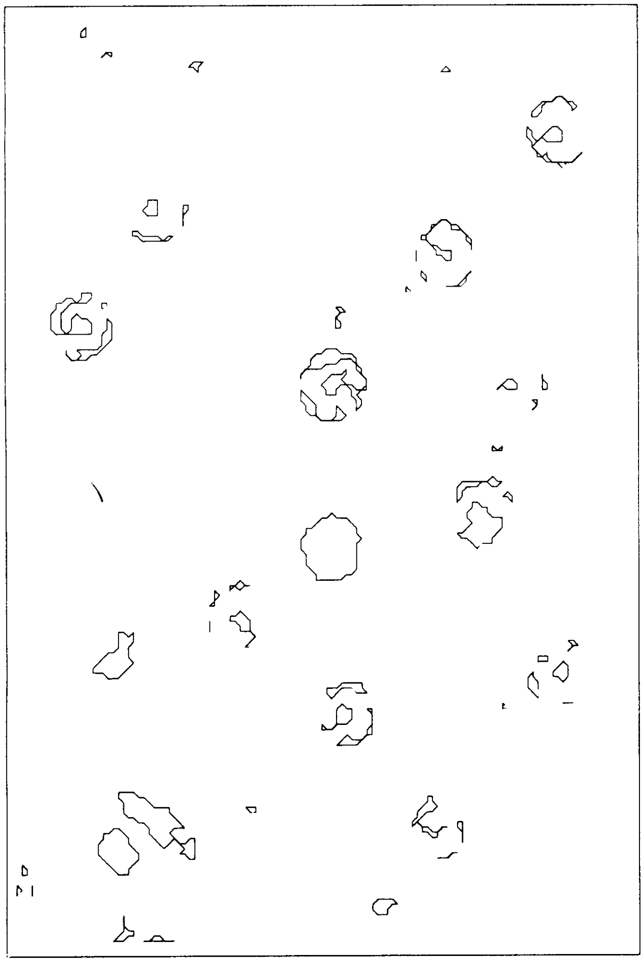

Fig. XI-20.

Fixed-threshold contour plot of the bright regions in Fig. XI-14.

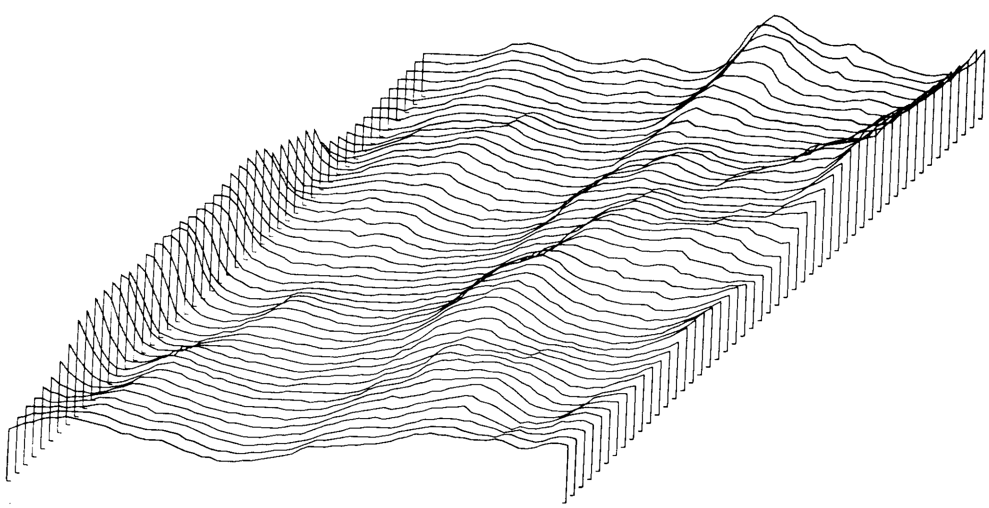

Fig. XI-21. Plot of picture brightness along lines perpendicular to and bisected by the vector shown in Fig. XI-19. Plot is 65 points in x and 50 points in y.

To do this, the user defines a vector on the display as shown by the crosses in Fig. XI-19. A plot of the brightness distribution on contours either parallel or perpendicular to this vector is then drawn. Figure XI-21 shows the brightness levels of points on contours perpendicular to the vector defined in Fig. XI-19. As can be seen, the plot gives a useful perspective indication of the brightness distribution across the indicated cell wall boundary.

(g) Filtering

In order to enhance boundaries in pictures, it is often desirable to prefilter the picture before the analysis is done. Routines which have been implemented to do such filtering allow the operator to define, through the teletype, a symmetrical filter with the desired weights. This filter is then convolved with the desired section of the picture to produce a new filtered picture.

3. Summary

I have given an overview of a highly interactive program for extracting and displaying in various manners information in pictures. The program is now being used in conjunction with several image-processing problems, and has been found useful in two respects. First, it allows the user to extract quantitative information about the particular problem

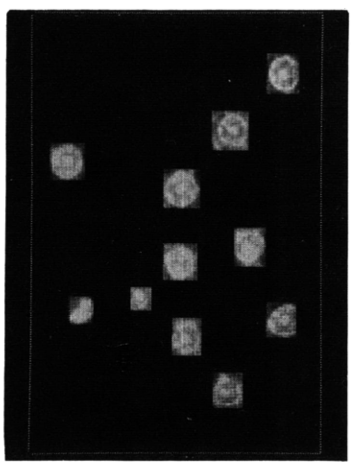

Fig. XI-22. Photograph of regions in Fig. XI-14 that were found to contain nuclei.

with which he is concerned to aid in deciding how to proceed with the necessary image processing. Second, it has been used to interface with various other processing routines to input data for them and to observe the results of the processing. As an example of this interaction, Fig. XI-14 was scanned by this program and saved on disc. Another program that searches for nuclei was then used to analyze the picture and produce a table containing the nuclei that were found. This table was then read in by the program described here, displayed on the photodisplay and photographed. The nuclei that were located are shown in Fig. XI-22.

D. Hartman

F. CHARACTER RECOGNITION: PERFORMANCE OF HUMAN COMPUTERS

1. Introduction

The philosophical difference between human perception and computer recognition of printed characters seems to depend on the researcher's bias. The cognitive psychologist maintains that the distinguishing characteristics of the entire stimulus give rise to the percept with no single attribute being either necessary or sufficient; in contrast, the engineer views pattern recognition as extracting various mathematical measures from the stimulus by using various transformations. Although these two approaches are not necessarily antithetical, there is a fundamental disagreement about whether the ultimate pattern-recognition algorithms should be based on psychological features, whatever they may be, or on extensive mathematical operations that perform the desired task with high statistical accuracy (Blesser and Peper[1]).

The computer programmer is more than willing to incorporate the knowledge of the psychologist into the programs if he can explain in step-by-step fashion which stimulus features, or their relationship, give rise to the psychological label. Unfortunately, the locus of high information density in a given letter can only be determined after the character is recognized. At present, we know of no way of specifying a priori the location of the labeling information. In a very real sense, the most difficult part of the recognition process is the beginning. The computer has in its memory an exact point-by-point mapping of the original optical stimulus and it must then decompose this highly redundant information into a final decision. Recognition based on the largest possible group of these points is nothing more than the template matching algorithm; namely, if all points in the stimulus coincide with the computer's stored model, then the character is correctly recognized. This gives the appearance of being a "gestalt," in that the entire character is used at one time to make a judgment, but it requires that the character set be highly defined with only one size, style, font, and minimum of noise; and it is not the pattern or organization of the character that gives rise to a correct judgment but an equally weighted point-by-point comparison. This is totally unsuitable for a system which, in the limit, should approach human performance.

The feature-extraction technique is a less restrictive and perhaps more powerful algorithm. In this method, local attributes of the stimulus are recognized independently and the resulting encoding is used to specify the letter. A "B" might thus be represented as the attributes: left-hand full vertical with two right-hand touching closures, one above the other. This compact and most general type of description requires, however, that the psychologist tell the programmer how to find these attributes from the point-by-point representation. The difficulty in this approach can be seen from the following examples. Is the part of the letter shown in Fig. XI-23 the serif of the top of an "I" or the crossbar on a sans serif "T"? This kind of decision can only be made by considering the rest of the letter. That is to say, the local attribute cannot be assigned a value out of the context of the remaining attributes. Similarly, is the line shown in Fig. XI-24 a pseudo vertical of italics "P" or the oblique line

Fig. XI-23.
Illustration of feature ambiguity without complete context. This could be the top serif of an "i" or the crossbar on a sans serif "T".

Fig. XI-24.
Illustration of feature ambiguity without complete context. This could be the pseudo vertical of an italic "P" or the oblique segment of a "V".

of a "V"? Thus, by using local features, the computer has a more compact and relevant description, but it is difficult to detect these features without some kind of normalization routine. A typical computer program overcomes, or attempts to overcome, these difficulties by specifying all of the possible ambiguities that might be encountered. This represents a sequence of special cases which might have to be dealt with under the specified condition of operation.

In this experiment, we attempted to determine how well human subjects could perform the recognition task when they were restricted to a sequentially derived point-by-point representation of the character. In other words, when a subject was made to feel as limited as a computer, what kind of strategies would he use. We hope that the fundamental structure for new character recognition algorithms might be one of the by-products of this investigation.

2. Methodology

Subjects were seated in front of the apparatus, as shown in Fig. XI-25, which contained an opaque movable plate covering the letter that was to be recognized. The letters, taken from the Prestige Elite 72 typewriter font and magnified by a factor of 40, were viewed through a 1/4-in. hole in the opaque plate. The diameter of the hole corresponded to approximately one-half of the average width of the letter

Fig. XI-25. Experimental apparatus.

stroke. An example of a letter is shown in Fig. XI-26. Movement of the plate was recorded to show the strategy used by the subject as he uncovered the information

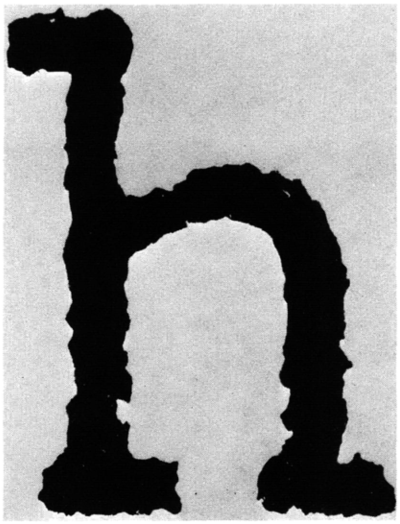

Fig. XI-26. Example of a stimulus letter enlarged from a standard typewriter. Approximate dimensions 6" × 5".

about the letter's shape. The eleven volunteer subjects, recruited from the laboratory staff, were instructed to look through the peephole in the plate while moving it over the letter. At the same time, they were asked to "think out loud" or to introspect the conscious mental strategy and the resulting perception. The technique is similar to that developed by Duncker[2] in which subjects were instructed to continuously verbalize their steps in problem solving. After each identification of a letter, the experimenter questioned the subject on the method that he used to identify the letter and reminded the subject to verbalize as much as possible. These comments were tape-recorded; the pentagraph output, used to record the movement of the hole, did not give reliable insight into the sequence of steps.

3. Results

The process of recognizing characters under these restricted conditions is characterized by two stages: initial acquisition of letter boundary; and acquisition and idenfication of the letter.

a. Initial Acquisition

The peephole was started initially from the upper left-hand corner of the photographic paper on which they were printed. Most subjects scanned diagonally downward toward the lower right-hand corner even though this corner was not visible. In this initial sweep, they successfully acquired the letter when the area in the peephole showed the black ink of the letter rather than just the white background. Only one subject used a pure raster scan in which the hole was moved horizontally and gradually lowered. In all cases, the subject has to have some preconscious notion of what to look for, otherwise he will not perceive the black-white boundary as part of the letter. For example, one subject kept scanning the page because he expected the letter to be completely visible through the small hole. Only after the experimenter pointed out that the letter was much larger did he perceive the black-white boundary as part of the letter. After the letter had been localized, the acquisition strategy was then used.

b. Acquisition and Identification of the Letter

Once the subject had localized the letter, he had to move the peephole in such a way as to extract sufficient information to make a judgment about the letter's identity. Thus, the subjects could perform a contour trace around the outside of the letter, raster scan across the height and width of the page, scan the interior of the line segment, or use any other data-gathering approach. All of these strategies, or in computer terms "algorithms," require subroutines to actually perform a task such as contour tracing. Which way should the hole be moved to follow the contour? Unlike the computer, however, the subjects could change their strategy as they had gained partial information about the letter. Three kinds of techniques were basically used.

<u>Method A</u>

The subject traced the whole outer contour of the letter and tried to retain "interesting" features of the trace, such as verticals, loops, ends, intersections, and so forth; for example, "There is a loop in the lower right-hand corner with an arm in the upper right." Such a description must clearly refer to the letter "d". This either became apparent to the subject intuitively or resulted from a process of elimination which revealed this to be the only letter satisfying the description. In this method, the subject first tried to preserve the continuously developing topographical representation until all of the data had been gained from the completed contour trace. It is important to realize that for most subjects the data are being continuously reduced to "feature attributes" rather than preserving a complete image of the letter with all unimportant serifs, noise, and font-dependent characteristics.

<u>Method B</u>

This method is similar to Method A, except that the subject continuously tested hypotheses as he was acquiring the data. Once the subject had identified a feature, he could separate the alphabet into likely and unlikely candidates for fitting the data. In the example shown in Fig. XI-27, the subject rapidly hypothesized that it must be either a "c" or an "o" based on the fact that the top of the letter was found to be curved. This ambiguity was quickly checked by continuing the scan while checking for the presence of a gap that would have indicated it to be "c" or the lack of a gap for an "o". Actually, the

Fig. XI-27. Pentagraph output of the trace used in tracing the letter "c" by the hypothesis testing method.

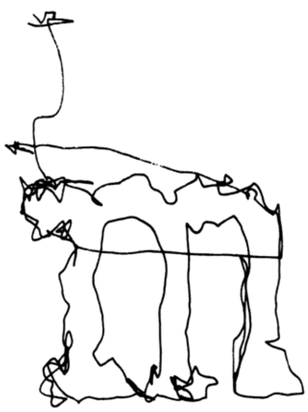

Fig. XI-28. Same as Fig. XI-27, except that a contour trace and a final hypothesis test are used to verify that it is an "m".

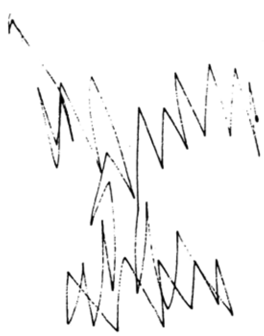

Fig. XI-29. Same as Fig. XI-27, except that a zig-zag tracing across line thickness of the letter "r" is used.

Fig. XI-30. Same as Fig. XI-27, except that a hybrid method of both contour and zig-zag is used for the letter "k".

letter might have been an "e" which would have fit the "c" test, namely, a gap. This method is characterized by the ability to perform a very rapid contour trace if the letter were guessed correctly. The contour followed was in fact sometimes at the black-white boundary of the letter and sometimes in the middle of the black line. Similarly, as shown in Fig. XI-28, the subject rapidly acquired the character and tested it for an "m" by drawing a line through the three legs. No other letter has the three legs. It seemed for all subjects that certain letters have fairly unique shapes and are easily guessed from very little information. The shape of a letter at its high information-density point almost always suggests one or at most a few particular letter.

Method C

This method differs from the first, in that the information subroutine contains a zig-zag sweep across black regions, that is, going from the white-black boundary to the black-white boundary. The example shown in Fig. XI-29 was produced by a subject whose scan was 1 1/2 times the thickness of the letter stroke. This technique, in comparison with contour tracing, allowed the subject to judge whether the line segments were curved, straight or intersecting with other curved lines. Using this method, the subject could get a much more complete picture of the local shape and could filter out noise by providing local context. The resulting features were then identified as in either Methods A or B. Figure XI-30 shows a hybrid method.

4. Observations

Although the discussions have emphasized the difference in the strategies, it should be apparent that they are all very similar, and differ, for the most part, in the amount of risk that the subject takes by making an early guess. The subjects are trading-off two opposing tendencies. On the one hand, there is the desire to make an early correct judgment so as to be able to perform confirmatory tests and finish the contour, or its equivalent, with a minimum of effort. It is clearly much easier to be asking "Does this additional datum fit a 'b' or not," rather than trying to encode local attributes into features. Once a guess is made, however, the subject has formed a psychological "set," and is very likely not to give up an incorrect hypothesis until the evidence is overwhelmingly against his guessed letter. On the other hand, a more secure data acquisition with delayed judgment, such as completely tracing the entire letter, is inherently more vulnerable to the effects of noise (line segment variations), an unexpected serif (most people are unaware of where the serifs are located), a break in the letter (the continuing side of the gap is completely missed), or forgetting the existence of an intersection (only one leg of an intersection can be traced at one time). Any kind of error can result in a set of features that do not fit together. The sooner the subject was able to arrive at a hypothesis, the easier was his task, since the strategy became confirmatory rather than acquisitory. Previous to the hypothesis, the subject must detect features that are inherently difficult because he does not have any Euclidean sense of space or distance. Although it seems that the subjects somehow mapped a two-dimensional feature space in their heads, it remained topologically elastic.

The recognition of the letter was not only dependent upon the subjects' strategy but it was also a function of his psychological "set." The subjects appeared to define an archtype variant of each letter; also, they seemed to have strong tendencies toward a select group of preferred letters. For example, if the subject expects that none of the letters will be repeated, the second attempt to recognize a letter takes him much longer. This is shown in Fig. XI-31 where the letter was retraced many times before recognition resulted. This is the classical phenomenon of set and negative perseveration (Uznadze[3]). In this example, the subject concluded that an "h" might be an "a" placed sideways. The massive serif and the very short vertical stem compared with the large lower circle just did not match his own reference topology of any letter. One Japanese subject identified the letter "j" as an inverted "c" which he said was very similar to the Japanese character "コ" of Katakana and "つ" of Hirakana. Thus the large serif was incorporated as a feature, and the resulting character was, in his character set, legal.

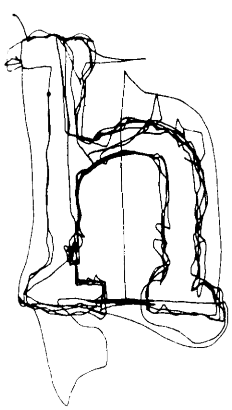

Fig. XI-31. Pentagraph output using the contour-tracing algorithm in which the subject would not accept that it was a letter "h" because that letter had already been presented. Note the many contour tracings acquiring the same information many times.

As the subjects became more familiar with the character set they had less trouble judging the significant letter fragments. Understandably, it took much longer to identify the first letter before the subject had a relative filter for the size, shape, line thickness, serif size, and line variations of the letter. In particular, when the subject was not sure of the relationship between serifs and letter fragments recognition was much slower and often erroneous. The differential judgment between a straight line and a slow curve (both with noise) can only be made by perceptual integration along the curve. One subject, during the recognition of his first letter, as shown in Fig. XI-32, was in the process of setting his filter to separate psychological noise from features.

All of the data-acquisition strategies mentioned have the interesting property that the subject had much more data available than he could profitably use. In almost every

Fig. XI-32. Pentagraph output for a subject's first experience in identifying a letter. The repeated tracing of the top serif illustrates the process of setting a psychological filter to determine whether this is a significant part of the letter.

case, an observer could guess the letter correctly by looking at the tracing being produced by the pentograph before the subject could. The data were there if they could be integrated into a unit. This distinction between the integrated data available to the observer and the feature-extracted data stored by the subject is the same distinction made when comparing a computer algorithm and human perception. We still do not know what it means to have an integrated representation of the stimulus in a computer format.

5. Future Experiments

A better understanding of how filtering techniques are created and used by subjects will be investigated by using a character set made up of mixed sizes and fonts. Subjects will thus not be able to normalize on the type font, but must reset the distinction between noise and feature with each new character. Other experiments in which extensive practice is given might help to determine the optimum strategy under the sequential data-processing restriction.

6. Conclusions

This experiment demonstrated a methodology for investigating human character recognition under the condition of sequential point-by-point data acquisition. It is clear that subjects do not store the information in its raw form but reduce it to some set of features or psychologically relevant attributes. At some point sufficient data have been gathered for the subject to formulate a hypothesis about a letter's identity.

It appeared that pure contour tracing is both inefficient and sometimes erroneous when there are breaks in the letter or loose fragments. The zig-zag method gave more local context, and might be useful for computer subroutines. Moreover, there is the suggestion that recognition algorithms might be divided into two preliminary stages: in the first, a limited number of guesses are made based on a preliminary analysis, in the second, the guesses are checked by using confirmation algorithms; for example, a "b" must have a left-hand vertical and a lower right-hand closure.

B. Blesser, E. Peper

References

1. B. Blesser and E. Peper, "Relevance of Psychology to Character Recognition," Quarterly Progress Report No. 97, Research Laboratory of Electronics, M. I. T., April 15, 1970, pp. 150-152.
2. C. Duncker, On Problem Solving (American Psychological Association, Washington, D. C., 1945). (Translated by Lynn S. Lees.)
3. D. N. Uznadze, The Psychology of Set (The Consultants Bureau, New York 1966). (Translated by Basil Haigh.)